In: Optimization in Polymer Processing ISBN # 978-1-61122-818-2
Editor: A.Gaspar-Cunha, J. A.Covas, pp.1-35

Chapter 5

POLYMER EXTRUSION - SETTING THE OPERATING CONDITIONS AND DEFINING THE SCREW GEOMETRY

José António Covas, António Gaspar-Cunha
Institute for Polymers and Composites/I3N, University of Minho, Campus de Azurém, 4800-058 Guimarães, Portugal

Key words: Extrusion, optimization, operating conditions, screw design.

1 Introduction

Plasticating extrusion (i.e., the conversion of solid pellets or powder of a polymer system into an homogeneous melt that is continuously pushed through a shaping die) is a major plastics polymer processing step:

- Extrusion lines, comprising one or more extruders, a shaping die and downstream equipment, are used to manufacture a wide range of mass consumption plastics products (e.g, profiles, pipes & tubing, film & sheet, wires & cables, filaments, fibers, non-wovens).

- Compounding lines, are not only used for additivation (i.e., incorporation of additives such as lubricants, processing aids, plasticizers, anti-oxidants, UV stabilizers, impact modifiers) and pelletization (usually preceded by melt mixing and devolatilization), but also to prepare/create advanced polymer

based systems, such as highly filled compounds, nanocomposites, polymer blends, hybrid materials, thermovulcanizates, or modified functionalized polymers. In several of these examples, chemical reactions take place simultaneously with processing, i.e., the extruder is also utilized as a continuous reactor. Some commercial polymers can also be synthesized and pelletized continuously in an extruder.

- Plasticating extruders are the core unit of some other important polymer processing technologies, such as injection molding and blow molding, and of a few rapid prototyping methods. For instance, in injection molding the screw can also move axially, which initially lets melt to accumulate at its tip and subsequently injects it into the mould cavity.

- Finally, it seems worth noting that plastics extrusion technologies have been successfully applied in other industries, particularly for the processing of food, pharmaceuticals and ceramics.

Modern extruders consist essentially of an hollow barrel, which is kept under a set temperature, inside which one or more Archimedes-type screw(s) rotate(s) at controllable constant speed (thus, the machine comprises also a motor, a speed reduction gear, heaters, sensors and a control system). The geometry of these machines can vary widely, from single screw extruders with a screw having a constant square pitch, to multi-screw machines of intricate design. In industrial practice, single screw extruders are the most popular, although the screw profile can be relatively complex. Intermeshing twin screw extruders are also quite frequently used, both in counter- and co-rotating modes, the former being mostly used for PVC extrusion and the latter for compounding operations.

Generally, the solid polymer (in pellet or powder form) is supplied to the screw channel either by gravity flow from a hopper or by a feeder set at a prescribed rate. The solid is dragged along the screw and melts due to the combined effect of conducted and dissipated heat. This (highly viscous non-Newtonian) melt is subsequently homogenized (via both dispersive and distributive mixing), pressurized and forced to pass through the die, where it is shaped into the required cross-section, before being quenched. It is clear that the performance a given extruder will depend on a number of factors, including the polymer properties (thermal, physical and rheological), the operating conditions (screw speed and barrel temperature profile) and machine and die geometries [1-5].

Two major practical topics concerning extrusion consist in setting the operating conditions and/or the screw(s) configuration yielding the best process performance for the manufacture of a certain product. Traditionally,

this is solved based on empirical knowledge, coupled to a trial-and-error procedure, where tentative extrusion experiments, or machining of screws, are performed until satisfactory results, *i.e.*, the desirable performance, are obtained. Process modeling may assist this endeavor, by eventually decreasing the extent of the experimental effort, but it does not change its procedure. Indeed, extrusion modeling software solves the *direct problem*, i.e., it predicts the thermal and flow characteristics inside the extruder for a specific set of material properties, operating conditions and machine geometry. However, setting the adequate operating conditions, or screw geometry, involves solving the *inverse problem*, whereby the governing process equations are solved in order to the operating conditions or geometry, respectively, the thermal and flow characteristics being prescribed by the user [6]. Unfortunately, this is an ill-posed problem, due to the lack of unique connection between cause and effect.

Instead, setting the adequate operating conditions, or screw geometry, can be assumed as an optimization problem, where the performance - to be maximized - is measured by a number of relevant objectives. This is equivalent to a multi-objective problem that, given its typology, can be solved adopting a methodology based on Multi-Objective Evolutionary Algorithms (MOEA) [8, 9]. The procedure requires a method of quantifying the extrusion performance as a function of the input variables (material properties, operating conditions and system geometry), taking into account the relevant physical and thermal process phenomena. Since plasticating extrusion encompasses a number of individual process steps (namely solids conveying, melting and melt conveying) where those phenomena are distinct, each has to be described by specific forms of the governing equations (mass conservation, momentum and energy). The global modeling program takes in the proper sequence these numerical routines, which are linked by appropriate boundary conditions, together with constitutive equations describing the material rheological and thermal responses [1-4, 7].

The present chapter discusses the optimization of single and co-rotating twin-screw extruders [10-14]. It starts with a presentation of process modeling routines that is followed by a discussion of optimization algorithms that can be successfully adopted. Two case studies, each dealing with one type of extruder, are introduced, and optimization results are presented and discussed.

2 Modeling

2.1 Single Screw Extrusion

Figure 1 illustrates the typical layout of a standard single-screw extruder. The heater bands surrounding the barrel allow setting an axial temperature profile. The die is coupled to one end of the barrel, while the raw material is fed by a lateral hole at the opposite end, on top of which a hopper is fixed (the hopper usually consists of a vertical column with straight and inclined sections). The screw shown has a constant pitch but variable channel depth, thus generating three distinct geometrical zones. From hopper to die, one can identify a feed zone (with constant channel depth), a compression zone (with decreasing channel depth) and a metering zone (where the screw is shallower). For the same screw diameter, D and axial length, L, the length of each zone may vary, as well as the maximum and minimum channel depths, giving rise to quite different screw profiles. This, together with the possibility of changing the set temperatures and the screw speed, may produce quite distinct thermomechanical environments inside the machine, as local heat conduction, heat dissipation, velocity profile and residence time may differ substantially [1, 10].

As raw material is fed via the hopper, gravity-induced flow guarantees its transfer to the screw channel. Then, the material progresses along the screw due to friction dragging (basically, the material slides along the screw due to the friction created by the barrel inner surface) until it melts, as a result of the combined effect of heat transfer from the barrel (which becomes more efficient across the bulk as pressure grows) and mechanical energy dissipation (due to the mentioned friction forces). Melting is not instantaneous, but follows a relatively well-ordered mechanism that develops along several screw turns and involves the segregation of the melt from the surviving solids. In fact, the material melts mostly near to the inner barrel and accumulates in a melt pool that co-exists side by side with the solid bed. As melting progresses, the width of the former increases, while that of the latter reduces, until the process is completed. In the remaining of the screw channel, mixing (mostly distributive) and pressure generation develop, so that the polymer finally flows through the die at a given rate. Intensive experimental research demonstrated that this chain of events is quite general, although the characteristics and extension of each stage are obviously affected by the operating conditions, material properties and channel geometry. Consequently, as shown in Figure 1 (see succession of channel cross-sections), the overall plasticating sequence

can be sub-divided in various individual steps, also known as functional zones (these should not be confused with the screw geometrical zones, as their limits will depend on the intensity of the thermo-mechanical environment) [1-3]:

i) *solids conveying* in the hopper;

ii) *drag solids conveying* in the initial screw turns;

iii) *delay in melting*, due to the development of a thin film of melted material separating the solids from the surrounding metallic wall(s);

iv) *melting*, where a specific melting mechanism develops;

v) *melt conveying*, involving a regular helical flow pattern of the fluid elements towards the die;

vi) *die flow*.

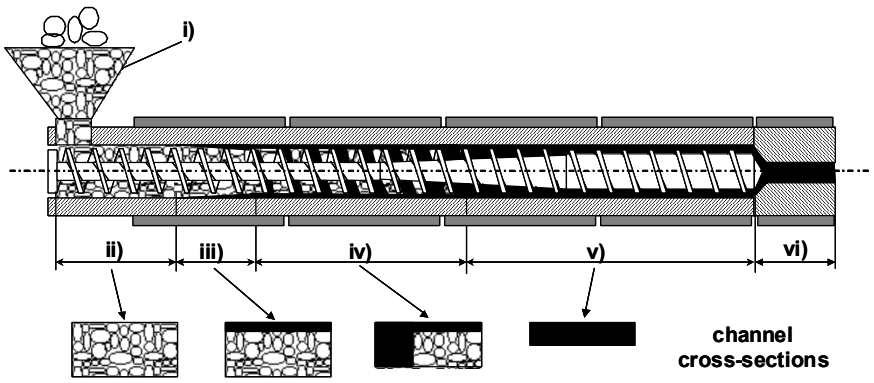

Figure 1. Physical phenomena in a plasticating single screw extruder (see text for the identification of the individual steps).

For modeling purposes, the hopper can be assumed as a sequence of vertical and/or divergent columns subjected to static loading, due to the significant difference between their free flow capacity and the effective discharge rate when mounted on extruders [5]. The corresponding vertical pressure profile can be computed adopting the analysis proposed by Walker [15], which is based on a force balance on an elemental horizontal bulk solids slice. The pressure at the bottom of the hopper represents the extruder inlet condition.

Modeling of drag solids conveying (Figure 2-*drag solids conveying*) is usually based on the classical assumption of the sliding of a non-isothermal

elastic solid plug between two plates with different friction coefficients. However, it should also take into account heat dissipation at all (screw and barrel) surfaces, as the solids temperature increases due to the contribution of conduction from the hot barrel and of friction near to the polymer/metal interfaces; heat convection develops due to the movement along the channel [16, 17]. The pressure generated can be determined from force and torque balances made on differential down-channel elements [16].

In the program used in the case studies discussed later, the delay zone is sub-divided into two sequential steps, following previous experimental evidence [1, 2]. Initially, the local higher temperatures and friction forces near to the inner barrel wall should favor the formation of a melt film at that same location (Figure 2-*delay in melting*-A). Afterwards, depending on local conditions, films of molten material may also form near to the screw channel walls (films B, D and E in Figure 2-*delay in melting*-B) by the same mechanism. For the first step, the approach of Kacir and Tadmor [18] was adopted to compute pressure and temperature profiles in the plug. The film thickness and temperature were obtained from solving the relevant forms of the momentum and energy equations, taking in heat convection in the down-channel and radial directions and heat conduction in the radial direction [10]. The second step was considered as a particular stage of melting, which occurs while the width of melt film B remains smaller than the channel height [19].

Various melting calculation schemes have been proposed in the literature, with the aim of relaxing some of the assumptions of the initial melting model proposed by Tadmor [1]. Lindt *et al* [19, 20] considered that the down-channel solid bed velocity is constant and that cross-channel flow exists. He presumed the simultaneous development of 5 regions (identified as A to E in Figure 2-*melting*), each being described by different forms of the momentum and energy equations, coupled to the relevant boundary conditions and force, heat and mass balances.

Melt conveying can be satisfactorily described as a two-dimensional non-isothermal flow of a non-Newtonian fluid, for example following the algorithm proposed by Tadmor and Klein [1]. As for the melt pool in the melting zone, the momentum and energy equations are solved, coupled to the relevant boundary conditions and to force, heat and mass balances. The extent of distributive melt mixing can be estimated from the growth of the interfacial area between two adjacent fluid components, as well as on their average flow residence time. Since that variation is proportional to the total shear strain, the latter can be used as a simple criterion to estimate the average degree of

mixing [21]. Here, a weighted-average total strain function, WATS, will be computed [10, 21, 22].

Pressure flow in the die can also be described as a two-dimensional non-isothermal flow of a non-Newtonian fluid. Since the actual flow channel from the die inlet to the lips is often geometrically complex, it is helpful to sub-divide it in a sequence of shorter channels of uniform cross-section, where fully developed flow develops.

The global plasticating extrusion model used in this chapter for process optimization purposes links sequentially the above steps through appropriate boundary conditions, in order to assure coherence of the physical phenomena between any two adjacent zones.

After estimating an initial output from volumetric considerations, calculations are carried out along small down-channel screw increments (Figure 3). If the predicted pressure drop at the die exit is not sufficiently small (theoretically, it should be nil), the output is changed and a new iteration is performed. A more detailed description of this program is given in another report [10].

The results provided include the evolution of important process variables along the screw axis, as well as global values. For example, Figure 4 depicts the axial evolution of pressure and of the relative presence of solids (in terms of the ratio between the solid plug width, X and the channel width, W). Figure 5 is a radar plot presenting the influence of screw speed (the values of 20, 40 and 60 rpm were selected) on mass output, mechanical power consumption, axial length of screw required for melting, average melt temperature, degree of distributive mixing (WATS) and maximum viscous dissipation (ratio of maximum melt temperature to barrel temperature). The sensitivity of the process to changes in operating conditions is obvious, the same being valid for geometrical parameters. Moreover, an increase in screw speed produces an increase in mass output, but at the cost of extra mechanical power consumption, higher viscous dissipation (and melt temperatures) and lower mixing quality (generally, WATS deteriorates as the screw speed increases, since a shorter channel section becomes available for mixing, due to the gradual lower melting rates and shorter residence times). Therefore, defining the best operating conditions and/or screw geometry is only possible if a compromise is sought between the relative satisfaction of the above parameters.

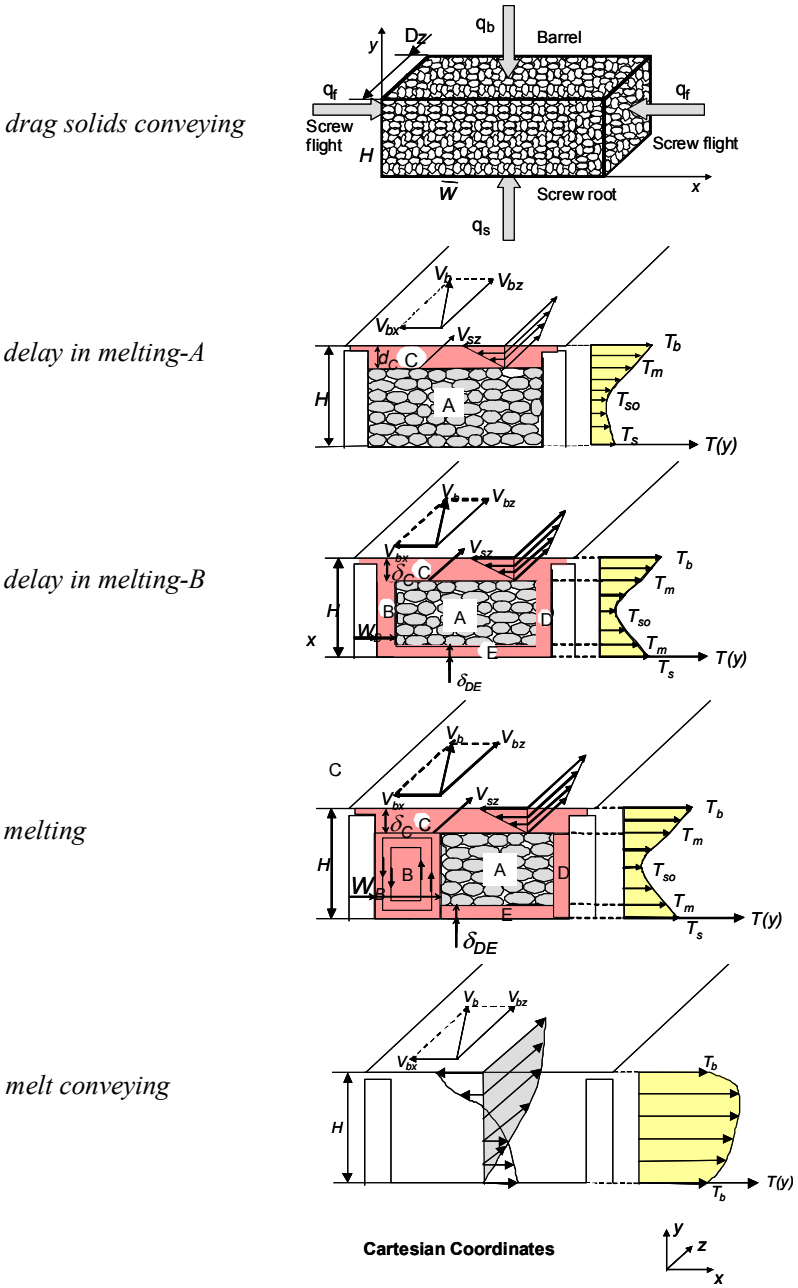

Figure 2. Illustration of the physical models of the various functional zones developing in plasticating single screw extrusion.

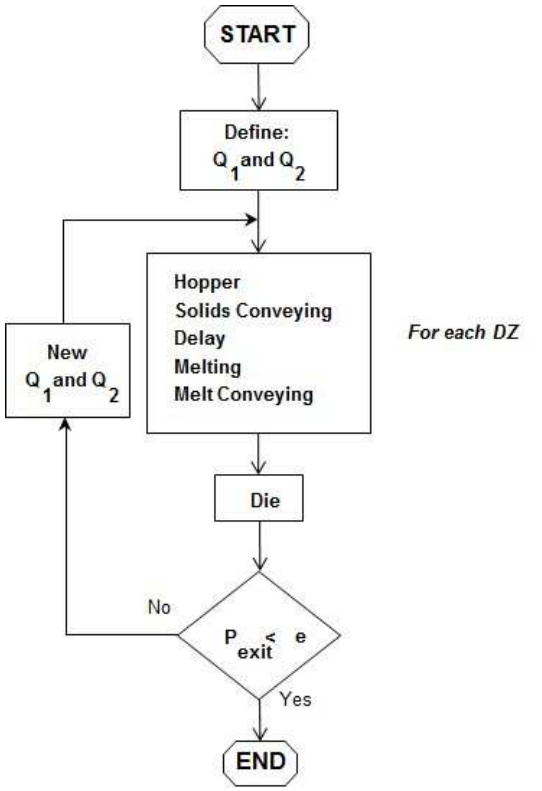

Figure 3. Flowchart of the global program for plasticating single screw extrusion.

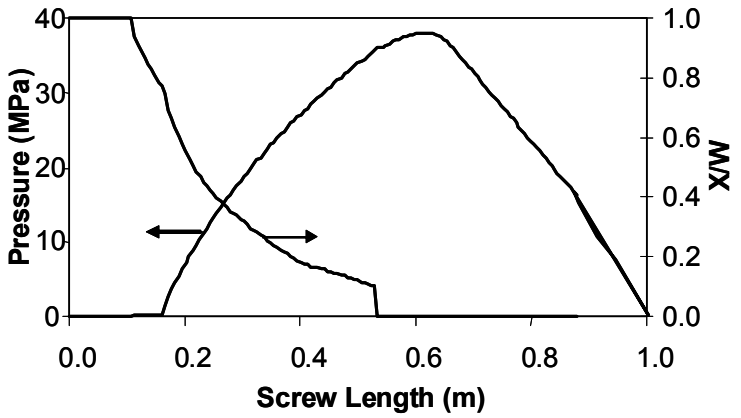

Figure 4. Axial profiles of pressure and relative presence of solids (at 60 rpm).

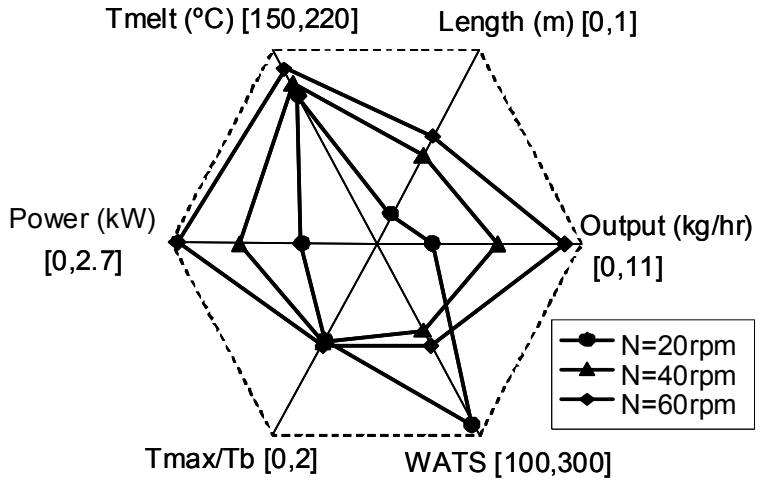

Figure 5. Influence of screw speed on various extruder responses.

2.2 Co-Rotating Twin-Screw Extrusion

As seen in the Introduction of the present Chapter, co-rotating twin-screw extruders are widely used for polymer compounding. In many industrial operations, different polymer systems are produced, possibly requiring different equipment configurations. One of the greatest practical advantages of these machines is their modular construction, valid both for barrel and screws. In fact, distinct short individual barrel segments may be fixed to each other (whose total length can thus be made shorter or longer, as appropriate), generating a barrel with apertures for, say, main feeding, feeding of a secondary polymer, feeding of a plasticizer in liquid form, feeding of a filler, vacuum-assisted devolatilization (i.e., for the removal of water or of low molecular weight species). Similarly, the screws are built from a varied number of individual elements that are progressively assembled along a shaft and finally fixed by a screw at the tip. Each of these elements is selected from a variety of geometrical types. Therefore, the process engineer can create screw profiles where the location of melting, the type and intensity of mixing and the average residence time can be relatively well controlled.

Another distinctive feature of these machines in relation to single screw extruders is the decoupling between output and screw speed. Single screw

extruders are typically flood fed, i.e., the raw material accumulates in the hopper, and thus the output essentially results from the difference between the drag capacity - which is linearly proportional to the screw speed - and the sensitivity to the die resistance. Co-rotating twin screw extruders work in starve fed mode, the feeding rate being determined by dedicated volumetric or gravimetric feeders. Thus, the screws work essentially partially filled, which means that for a given feeding rate, the screw speed can be used to adjust the intensity of the thermomechanical stresses.

Figure 6 shows a typical screw profile and schematizes the three types of individual screw elements that were used to build it. Each promotes distinct flow features, hence the global extruder performance is dictated by their overall action [4, 23]. Conveying, or right handed, elements drag material forward due to their positive helix angle; the higher the angle, the higher the conveying capacity. Left handed elements have a negative helix, thus impose a restriction to the flow that can induce local fully-filled flow conditions, heat transfer becoming more efficient and the flow pattern much more complex (again, the intensity depends on the helix angle). If the compound is still solid, melting can take place quite rapidly; in the case of melt flow, significant (dispersive/distributive) mixing and viscous dissipation may develop. Kneading blocks comprise a number of kneading discs (their thicknesses can vary) staggered at positive, neutral, or negative angle(s). Positive angles induce conveying capacity and promote some distributive mixing. Neutral angles have no drag capacity, hence the local flow residence time increases and both distributive and dispersive mixing take place. Negative staggering angles, like left handed elements, can be very efficient in terms of mixing. They can also be used for melting purposes [4, 23, 24].

While in the single screw extruder the material advances along the screw helical channel, in this type of machines it follows instead a figure-of-8 pattern along the channels of the partially-filled conveying elements of the two screws (for an observer positioned perpendicularly to the screw axis), since each screw interrupts the helical flow taking place in the adjacent screw. Once the material reaches a restrictive screw element, it must generate the pressure required to overcome the resistance created by the latter and continue its progression towards the die. Consequently, the material accumulates directly upstream of that restriction, filling up a few screw turns and spending longer local residence times before traversing it. The higher the restriction (defined by its geometry and length), the higher the pressure to be generated and the higher the number of screw turns upstream working fully filled. Thus, instead of a profile such as that depicted in Figure 4, axial pressure profiles in twin

screw extruders are much more complex (see example in Figure 9, to be discussed later).

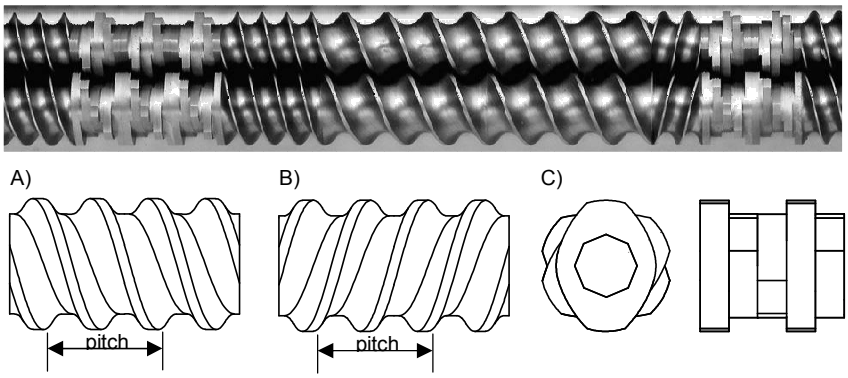

Figure 6. Co-rotating twin screw extruder. Top: close-up of a typical screw profile (www.coperion.com). Bottom: Types of screw elements included: a) conveying (or right handed) element; b) left handed element; c) kneading block.

Modeling of such a complex process in order to be able to predict the behavior of important process parameters (either as axial profiles or global levels) such as cumulative and local residence times, pressure, power consumption, average strain, specific mechanical energy, average shear rate, or fill ratio, requires simplifications both in terms of geometry and flow characteristics. The former will not be discussed here. As for the latter, as for the single screw extruder a number of sequential functional zones will be also considered here [4, 25-27] (see also Figure 7):

1) *solids conveying without pressure*, in the initial screw turns, upstream of the first restrictive element. One would expect that the incoming material remains relatively cold along these earlier screw turns, due to the weak heat transfer and generation capacities associated with flow in partially filled channels. Thus, only the residence time and the fill ratio are computed, which depend on operating conditions and geometry [26].

2) *solids conveying under pressure* - due to the presence of the first restrictive element, the material fills up a few channels upstream and pressure is generated to overcome the restriction imposed. The solid polymer quickly forms a solid plug exposed to heat conduction at all surfaces.

3) *delay zone*, resulting from the creation of a melt film when the temperature of the polymer near to the barrel reaches its melting temperature.

The thickness of this film increases until a melt pool near to the active screw flight is formed.

4) *melting (with high solids content)* - melting is assumed to extend in two stages, according with experimental observations reported in the literature [28]; after the formation of a melt film at the barrel surface, as mentioned above, the voids between the closely packed solid particles become progressively filled with this melt, creating a solid-rich suspension that progressively evolves into a melt-rich suspension. Thus, in this first melting stage the solid plug is surrounded by melt films and a melt pool, which grows in size. This situation can be adequately described by the 5-zone melting model proposed by Lindt *et al*. [20] for single screw extruders, cited above.

5) *melting (with low solids content)* - when the quantity of melted polymer reaches around 50% of the total polymer present in each cross-channel section, it means that a transition from a solid-rich to a melt-rich suspension took place, as there is enough liquid to encapsulate the surviving pellets [28]. In terms of modeling, it is assumed that the solid plug instantaneously bursts into a uniform suspension of pellets in the molten polymer, the progressive decrease of the particle size being described by a particle dispersed melting model [28, 29]. For simplicity, particles keep a spherical shape during melting. Heat transfer and energy balances are performed for a single particle. In turn, melt flow is modeled by solving the momentum and energy equations while describing viscosity by the Carreau-Yasuda law for concentrated suspensions [28].

6) *melt conveying under pressure*, upstream and/or along restrictive zones.

7) *melt conveying without pressure*, along conveying elements and away from restrictive zones. Only drag flow is considered and pressure is nil. Performing a thermal balance where heat conduction from barrel and screw are taken in, it becomes possible to compute the melt temperature profile [26].

8) *die flow*.

Steps 2 to 4, 6 and 8 are conceptually similar to the equivalent ones for single screw extrusion and, accordingly, their modeling features are analogous. Also, as in the case of single screw extrusion, the individual models presented must be linked together in a global model using coherent boundary conditions [25], the general flowchart being shown in Figure 8. After defining the operating conditions (screw speed, output and barrel set temperature profile), material properties and screw and die geometries, calculations start at the first restrictive element. An iterative process is employed to determine the screw location, upstream of that restrictive element, where pressure generation is initiated. Assuming an initial position, the program computes, for small down-

channel increments, and until the end of the first restrictive zone, the evolution of pressure, temperature, mechanical power consumption, shear rate, viscosity, residence time and fill ratio. If the pressure is not nil, the initial position is changed. For this first restrictive zone, the eventual development of solids conveying, delay, melting and melt conveying is taken into account, whereas in the remaining only melt conveying (under or without pressure) are relevant. As computations progress towards the die, every time a restrictive element is detected (or the die itself) a new iterative procedure is started to locate the fully filled portion of the screw.

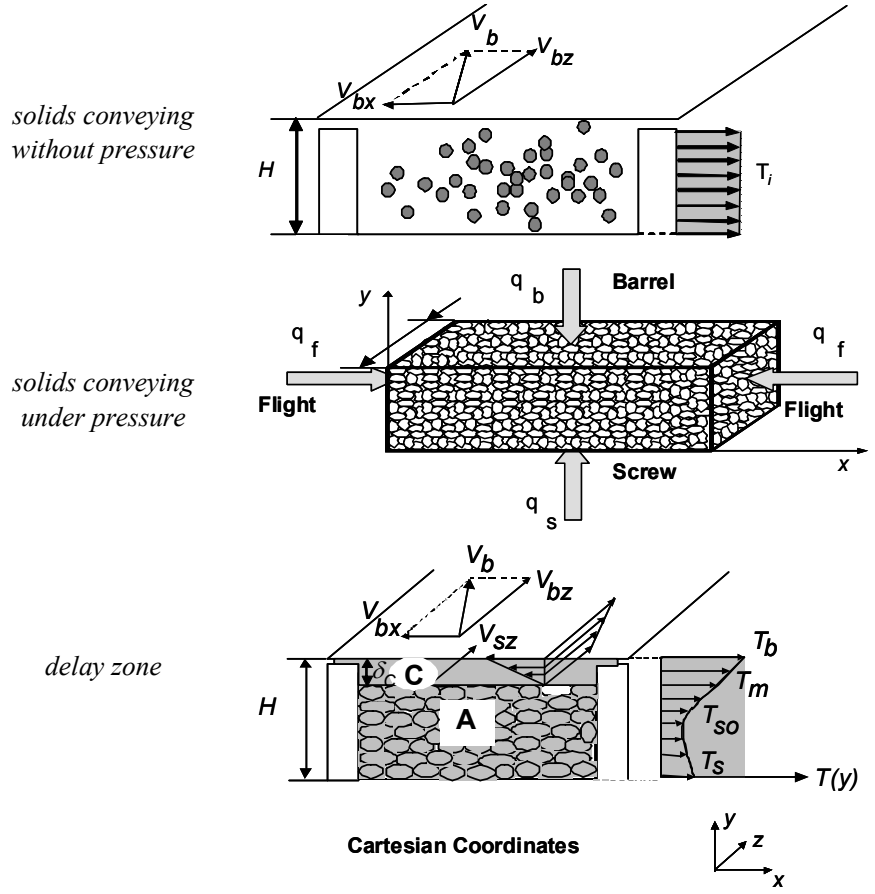

Figure 7. Illustration of the physical models of the various functional zones developing in plasticating co-rotating twin-screw extrusion.

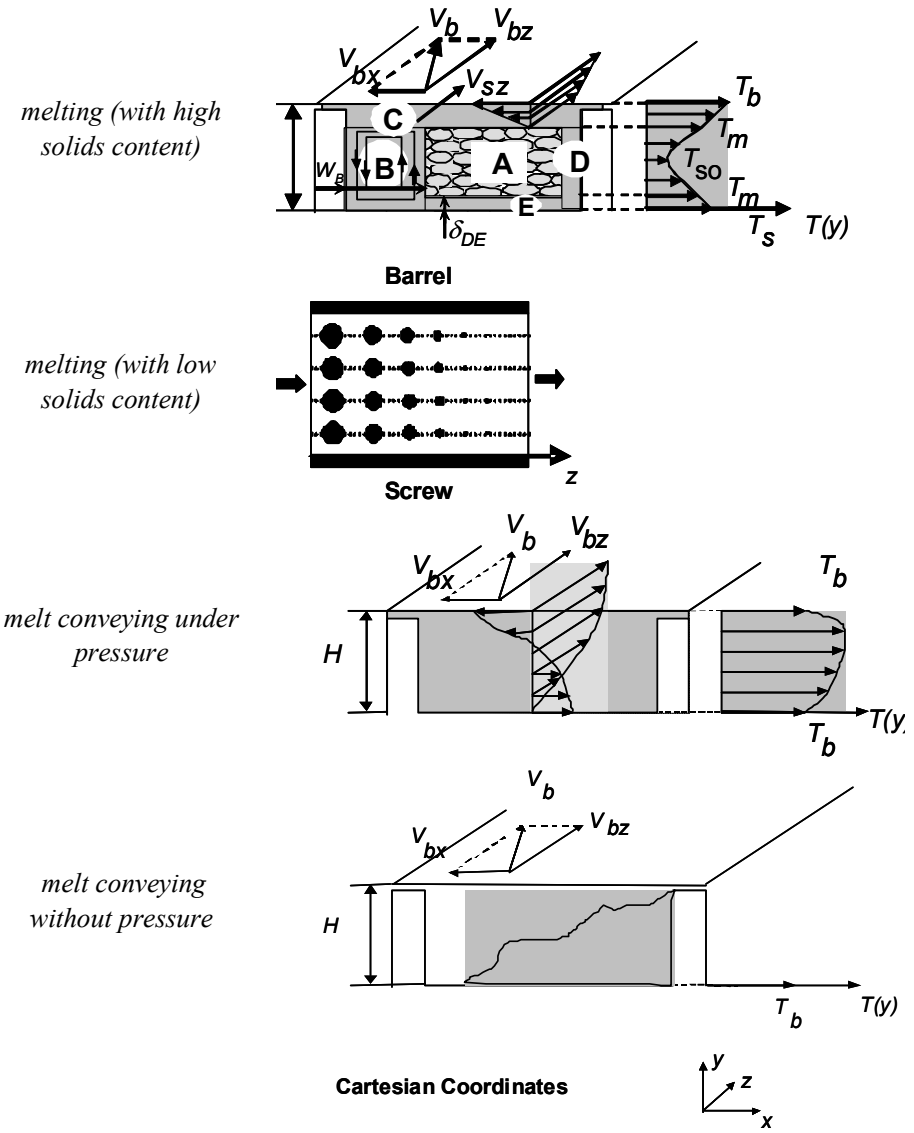

Figure 7. Illustration of the physical models of the various functional zones developing in plasticating co-rotating twin-screw extrusion (*continued*).

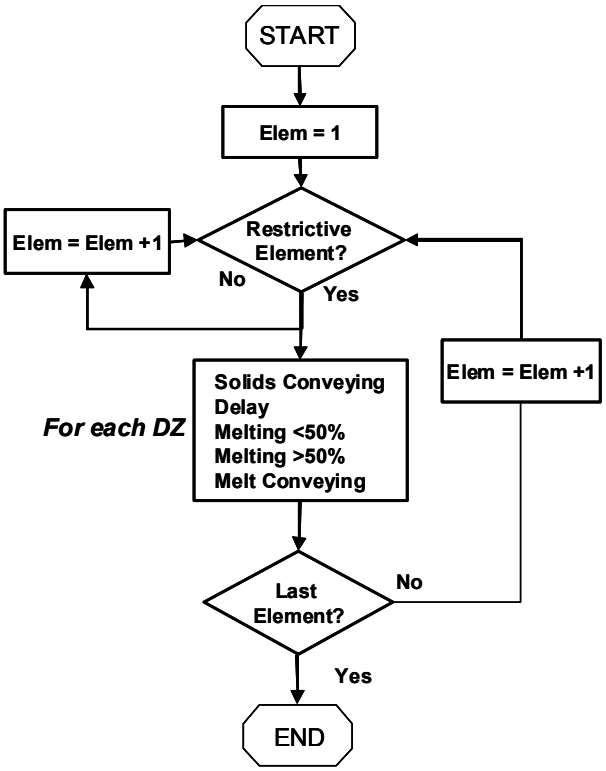

Figure 8. Flowchart of the global plasticating program for twin-screw extrusion.

Figure 9 shows some of the predictions of a computational routine encompassing the algorithms and individual process models presented throughout this Section. Figure 9a confirms the complexity of the axial pressure profile when compared to that of a single screw extruder (Figure 4). The three screw zones fitted with kneading disks or left handed elements, as well as the die, are flow restrictive, hence pressure must be generated upstream to be used up during flow along those elements. When the geometry of the first restrictive zone is modified but the remaining processing variables stay unchanged, only the local pressure profile is altered. The figure clearly shows that a kneading block staggered at -60º and a left handed element (LH) are the most restrictive, since the pressure generated is higher. Figure 9b shows the average melt temperature profiles. As expected, the melt temperature is higher

in the cases of the more restrictive elements, not only because the temperature starts increasing more upstream, but also due to higher viscous dissipation.

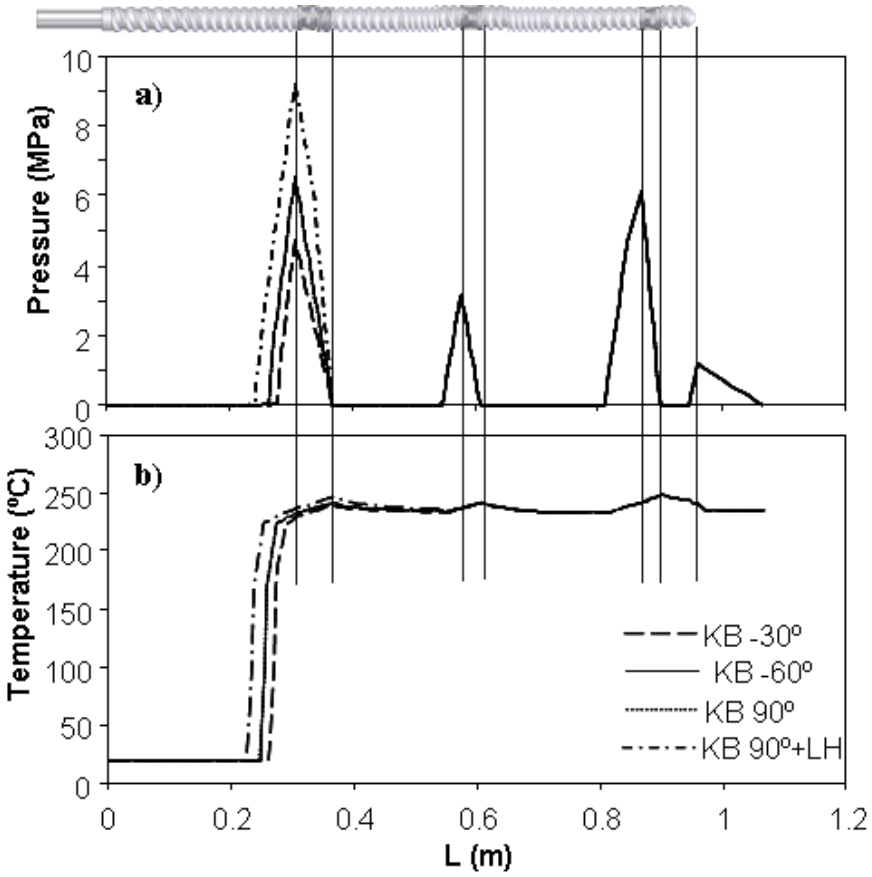

Figure 9. Axial pressure and average melt temperature profiles along screw and die for different configurations of the first restrictive flow zone.

3 Optimization Methodologies

3.1 Characteristics of the Optimization Problems

A key step in optimization is the identification of the characteristics of the problem that are susceptible to influence the selection of the optimization methodology and/or of the variables codification [30, 13]. In this respect, single and twin screw extrusion must be examined separately.

If a regular single screw extrusion operation is under progress, the process performance is determined by the operating conditions, namely screw speed (N) and set temperatures of the heater bands (T_b). The range of variation of the former is dictated by the characteristics of the machine's motor and reduction gear, whereas that of the latter must stay above the polymer melt temperature and below the onset of degradation. Within these intervals, these parameters vary continuously. If a new screw design is sought after, the geometric parameters can also be adjusted continuously within the prescribed ranges that are generally defined based on empirical knowledge (and related to the intensity and extent of the generated thermomechanical stresses). As seen in Figure 10a, an extruder screw can be defined by its diameter (D) and total length (L), by the length of the feed, compression and metering zones (L_1, L_2 and L_3, respectively) by the initial and final channel depths (or, equivalently, inner diameter ($D_{1)}$ and (D_3), respectively), by the flight thickness (e) and by the screw pitch (p).

In the case of a twin screw extruder, the operating conditions N, T_b, and mass output (Q) can also be made to vary continuously within feasible intervals. For example, Q can neither be set below the minimum capacity of the feeder, nor above the value that would induce flow in fully filled channels in the extruder. However, as explained above, in these machines screws are generally built by selecting elements from a set of available geometries and then assembling them in a certain sequence. If a screw is made of *n* elements and the aim is to define the best place for each one, there are *n*! possible combinations, i.e., a complex discrete combinatorial problem must be solved (this will be denoted as the Twin Screw Configuration Problem (TSCP)). Nevertheless, the problem of optimizing the geometry of individual elements would entail the continuous variation of the applicable parameters, again within a given interval.

The above optimization problems have a multi-objective character, since various objectives are to be considered simultaneously, some of them being conflicting. For example, increasing the screw speed of a single screw extruder

brings about higher outputs, but the quality of mixing may decline and the energy consumption raises. When assembling a screw for a twin screw extruder, a long kneading block improves mixing, but may cause excessive viscous dissipation. Evolutionary Algorithms will be used, more explicitly, a MOEA denoted as Reduced Pareto Set Genetic Algorithm (RPSGA) [11, 31], which was described in chapter 4. In turn, the following sub-section will explain how this algorithm can be modified in order to cope efficiently with the special characteristics of the TSCP.

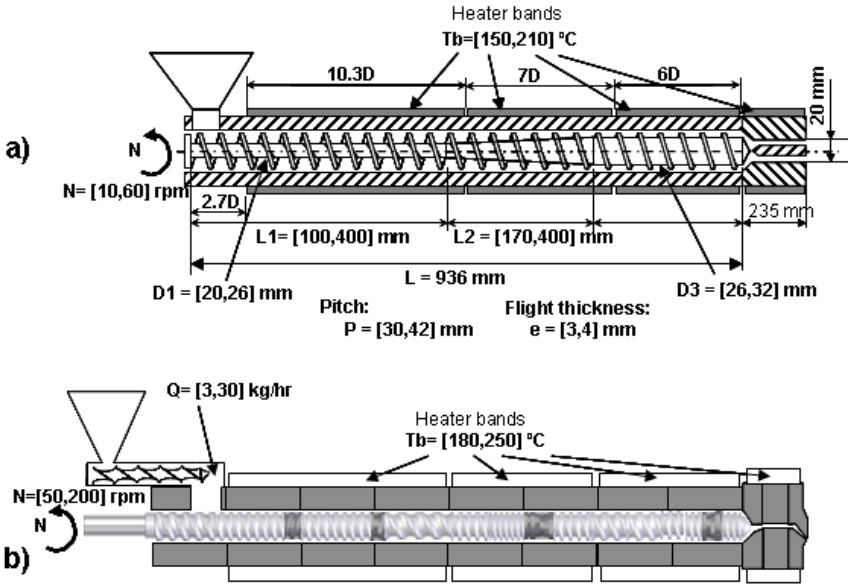

Figure 10. Operational and geometrical parameters to be optimized in (a) single and (b) co-rotating twin screw extruders. The values of the operating variables between brackets are typical for processing polyolefin's.

3.2 TSCP as a Sequencing Problem

The TSCP can be considered as a sequencing problem since, as discussed above, it consists in selecting a specific number of screw elements (of the type illustrated in Figure 6) from a wider set of available elements, and in defining their location along the screw axis, in such a way that the process performance

is maximized. Each solution consists of a given sequence of elements, whose performance may be quantified via the modeling routine.

Defining the TSCP in this manner enables the use of metaheuristics like MOEAs for process optimization. However, the original RPSGA requires some modifications. First, the decision variables are now discrete, representing the position of each screw element on the screw shaft. Second, a specific reproduction operator, incorporating crossover and mutation, must be used. The operator adopted, designated as inver-over, is able to make full use of the heuristic information contained in the population [31-33].

This type of formulation of the TSCP enables the application of other optimization approaches with the aim of accelerating the search procedure (given the significant computational cost of the modeling routine), such as Stochastic Local Search (SLS) algorithms, Multi-Objective Ant Colony Optimization (MO-ACO) and hybrid methods coupling MOEA and MO-ACO with local search procedures [32, 34].

4 Results and Discussion

4.1 Introduction

The multi-objective RPSGA presented in Chapter 4 will be used to solve problems involving setting the operating conditions and designing screws for the extruders represented in Figure 10 (while complying with the indicated ranges of variation).

A High Density Polyethylene, HDPE (grade ALCUDIA TR-135, manufactured by Repsol) and a Polypropylene, PP (grade ISPLEN PP 030 G1E, also manufactured by Repsol) will be used for the single and twin screw extrusion computations, respectively. The corresponding thermal, physical and rheological characteristics (the shear rate and temperature dependence of the viscosity are modeled by the Carreau-Yasuda equation) are summarized in Table 1.

The RPSGA was applied using the following parameters, which result from a prior investigation [10, 11]:

- 50 and 30 generations for the single screw and twin-screw optimization runs, respectively;
- crossover rate of 0.8;
- mutation rate of 0.05;
- internal and external populations with 100 individuals;

- limits of the clustering algorithm set at 0.2;
- number of ranks (N_{Ranks}) set at 30.

Table 1. Properties of the HDPE and PP selected.

			HDPE (ALCUDIA TR-135)	PP (ISPLEN PP 030 G1E)	
Density	Solids	ρ_s	495.0	560.0	$kg.m^{-3}$
	Melt	ρ	854.4	910.0	
Thermal Conductivity	Solids	k_s	0.186	0.21	$W.m^{-1.o}C^{-1}$
	Melt	k_m	0.097	0.18	
Specific Heat	Solids	C_s	2350	2480	$J.kg^{-1}$
	Melt	C_m	2535	2950	
Melting	Heat	H	$167x10^3$	$89.49x10^3$	$J.kg^{-1}$
	Temperature	T_m	119.9	169.11	^oC
Carreau-Yasuda law	viscosity	η_0	18000	3041.48	$Pa.s$
		E/R	10000	4023.29	K
		$\hat{\lambda}$	0.70	0.17	s
		a	1.70	1.82	
		n	0.30	0.35	
		T_0	463.15	493.15	K

4.2 Single Screw Extrusion

Table 2 presents the objectives to be considered in this study, the aim of their optimization and the prescribed range of variation.

Table 2. Optimization objectives, aim of optimization and range of variation for single screw extrusion.

Objectives	**Aim**	X_{min}	X_{max}
Output – Q (kg/hr)	Maximize	1	20
Length for melting – L (m)	Minimize	0.2	0.9
Melt temperature – T (ºC)	Minimize	150	210
Power consumption – P (W)	Minimize	0	9200
WATS	Maximize	0	1300

Seven distinct multi-objective optimization runs will be carried out, as illustrated in Table 3. Runs 1 to 4 deal with the simultaneous optimization of pairs of objectives linked to setting the operating conditions and, because they correspond to simpler optimization problems, they can be used by expert readers in single screw extrusion to check whether the optimization algorithm produces feasible optimized solutions.

Runs 5 to 7 tackle more complex optimization problems, where all the previous objectives are simultaneously considered. Run 5 corresponds to setting the operating conditions, run 6 to defining the screw geometry for a fixed operating point, whereas in run 7 the operating conditions and the screw geometry are to be jointly optimized.

Table 3. Optimization runs - single screw extrusion (Operating conditions: N, T_{b1}, T_{b2} and T_{b3}; Geometry: D_1, D_3, L_1, L_2, *Pitch* and e).

Run	**Decision Variables**	**Objectives**
1	Operating Conditions	*Q, L*
2	Operating Conditions	*Q, T*
3	Operating Conditions	*Q, P*
4	Operating Conditions	*Q and WATS*
5	Operating Conditions	*Q, L, T, P, WATS*
6	Geometry	*Q, L, T, P, WATS*
7	Operating Cond. + Geometry	*Q, L, T, P, WATS*

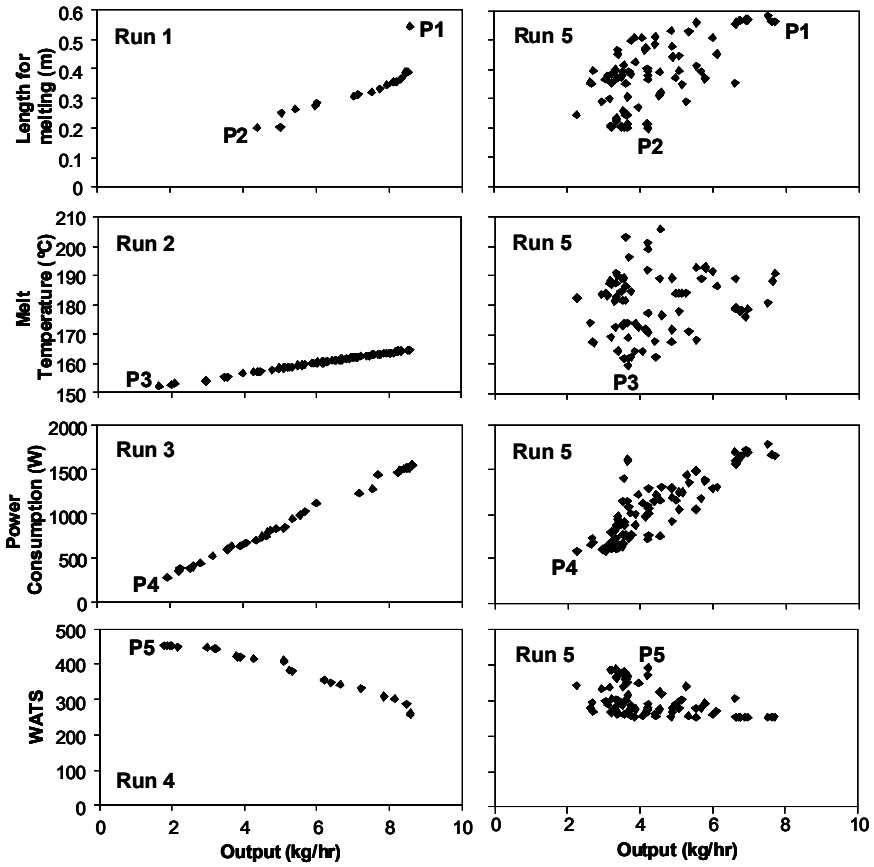

Figure 11. Comparison between the Pareto frontiers of runs 1 to 4 and run 5 - single screw extrusion.

Figure 11 presents the results obtained in runs 1 to 4 (Figure 11-left) and run 5 (Figure 11-right). When only two objectives are analyzed simultaneously, the algorithm converges to a line defining the trade-off between them in a two-dimensional space. The higher the output the slower the melting, the more important viscous dissipation becomes, the higher the mechanical power consumption and the lower the mixing quality. In the case of run 5, the algorithm works in a 5-dimensional space. For visual simplicity, only two-dimensional plots of various pairs of objectives are drawn. Some points that seem to be dominated in a specific representation are most likely

non-dominated in another 2-dimensional plot. Points *P1* to *P5* identify the best solutions that were found when optimizing each of the objectives considered. For example, point *P1* identifies the solution that maximizes the output, while point *P2* minimizes the length of the screw required for melting. Tables 4 and 5 present the numerical values of these 5 points for runs 1 to 5. For instance, the maximum output for runs 1 to 4 is 8.57 kg/hr, whilst for run 5 is attains just 7.69 kg/hr, a reduction of 10.2%. This is an obvious demonstration that the existence of several objectives (in run 5) may compromise the maximum values attained for the individual objectives. However, as shown in Table 6, which compares the values of the objectives attained in runs 1 to 4 with those obtained in run 5, in the case of the latter it was actually possible to achieve further gains in some objectives (namely, melt temperature and mechanical power consumption, to be minimized).

A similar comparison was made between runs 6 and 7 (see Table 3). Figure 12 illustrates the Pareto fronts for run 6. The clouds of points are again a sign that a compromise between all the objectives was made during the optimization. Table 7 presents the geometrical parameters obtained for the optimal solutions of run 6, while Table 8 shows the operating conditions and geometrical parameters for the optimal solutions of run 7. Finally, Table 9 compares the optimal processing conditions attained in run 7 with those for runs 1 to 4. All the objectives could be improved, except for the minimization of the length required for melting.

Table 4 - Optimal results for runs 1 to 4 - single screw extrusion.

Objective	**Operating conditions**				**Objectives**				
	N (rpm)	**T_{b1} (ºC)**	**T_{b2} (ºC)**	**T_{b3} (ºC)**	**Output (Kg/hr)**	**Length (m)**	**Tmelt (ºC)**	**Power Cons. (W)**	**WATS**
Max(Q)	59.4	210	196	199	**8.57**	0.544	206	1694	256
Min(L)	28.8	203	200	197	4.37	**0.200**	202	1051	406
Min(T)	10.7	150	202	150	1.64	0.323	**152**	296	297
Min(Power)	11.6	204	201	207	1.91	0.198	205	**276**	398
Max(WATS)	12.3	209	154	150	1.77	0.145	157	524	**454**

Table 5. Optimal results for run 5 - single screw extrusion.

Objective	Operating conditions				Objectives				
	N (rpm)	T_{b1} (ºC)	T_{b2} (ºC)	T_{b3} (ºC)	Output (Kg/hr)	Length (m)	Tmelt (ºC)	Power Cons. (W)	WATS
Max(Q)	54.2	188	170	177	**7.69**	0.562	191	1654	254
Min(L)	29.5	185	184	162	4.22	**0.201**	177	1292	392
Min(T)	25.4	151	188	157	3.66	0.215	**160**	1598	369
Min(Power)	14.7	170	178	189	2.26	0.246	183	**586**	342
Max(WATS)	29.5	185	184	162	4.22	0.200	177	1292	**392**

Table 6. Difference between the values of the Objectives of runs 1 to 4 and run 5 (as percentage) - single screw extrusion.

Objective	Output	Length	Tmelt	Power Cons.	WATS
Max(Q)	**-10.2**	-3.2	7.2	2.3	-1.1
Min(L)	-3.5	**-0.5**	12.5	-22.9	-3.5
Min(T)	123.0	33.4	**-4.8**	-439.5	24.4
Min(Power)	18.5	-24.7	11.1	**-112.3**	-14.2
Max(WATS)	138.5	-38.7	-12.7	-146.7	**-13.7**

Table 7. Optimal results for run 6- single screw extrusion.

Objective	L_1 (mm)	L_2 (mm)	D_1 (mm)	D_3 (mm)	Pitch (mm)	e (mm)
Max(Q)	131	259	22.1	27.9	38.7	3.1
Min(L)	101	183	22.0	31.7	32.2	3.3
Min(T)	168	301	21.8	32.0	37.0	3.5
Min(Power)	390	365	21.7	30.9	40.7	3.1
Max(WATS)	101	181	21.9	31.9	31.1	3.4

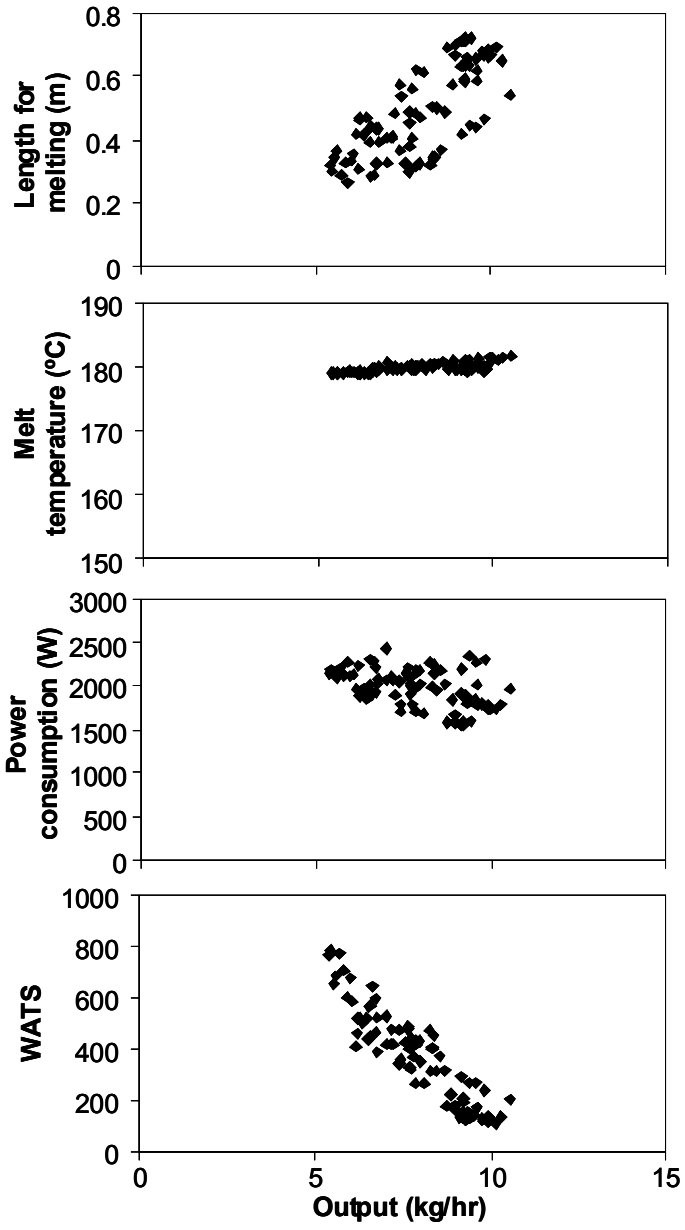

Figure 12. Pareto frontiers for run 6 - single screw extrusion.

Table 8. Optimal results for run 7- single screw extrusion- single screw extrusion.

Objective	N (rpm)	Tb1 (ºC)	Tb2 (ºC)	Tb3 (ºC)	L1 (mm)	L2 (mm)	D1 (mm)	D3 (mm)	Pitch (mm)	e (mm)
Max(Q)	58.1	189	198	172	174	266	23.3	27.3	38.1	3.5
Min(L)	24.1	207	195	177	143	305	24.2	26.8	37.6	3.3
Min(T)	19.7	152	180	156	204	248	25.0	31.1	36.2	3.1
Min(Power)	10.9	161	196	152	270	290	25.1	29.4	37.9	3.3
Max(WATS)	46.8	183	179	173	138	220	25.0	31.2	41.4	3.5

Table 9. Difference between the values of the Objectives of runs 1 to 4 and run 7 (%)- single screw extrusion.

Objective	Output	Length	Tmelt	Power Cons.	WATS
Max(Q)	**61.9**	-9.2	-0.9	-18.0	-39.8
Min(L)	32.2	**-27.9**	-12.7	46.8	-23.1
Min(T)	-5.3	-77.4	**1.0**	49.6	0.6
Min(Power)	8.5	-54.6	12.6	**36.1**	-22.2
Max(WATS)	63.6	-66.0	-5.8	-35.8	**20.5**

4.3 Co-Rotating Twin-Screw Extrusion

In the case of co-rotating twin-screw extrusion, three different objectives are considered: maximizing the average strain and minimizing the specific mechanical energy and the viscous dissipation (Table 10). Table 11 summarizes the basic screw configuration used. Three runs were performed: the first optimizing the operating conditions (output ranging in the interval [3-30] kg, screw speed ranging in the interval [50-200] rpm and barrel temperature ranging in the interval [180-250] ºC); the second optimizing the screw configuration, where the screw elements 1 and 2 (Table 11) were fixed and all the other are allowed to change their location; and the third were both the operating conditions and the screw configuration are optimized simultaneously. In all runs the three objectives shown in Table 10 are optimized concurrently.

Table 10. Optimization objectives, aim of optimization and range of variation for twin-screw optimization.

Objectives	**Aim**	***Xmin***	***Xmax***
Average strain – *AvgS*	Maximize	1000	15000
Specific mechanical energy – *SME* (MJ/kg)	Minimize	0.1	2
Viscous dissipation – *VD*	Minimize	0.9	1.5

Table 11. Basic screw configuration - twin screw extrusion.

Screw Element	**1**	**2**	**3**	**4**	**5**	**6**	**7**	**8**	**9**	**10**	**11**	**12**	**13**	**14**	**15**	**16**
Length (mm)	97.5	120	45	60	30	30	30	60	30	120	30	120	37.5	60	60	30
Pitch (mm)	45	30	KB -45º	30	-20	60	30	20	KB -60º	30	30	60	KB -30º	45	30	20

Figure 13 show the Pareto frontiers, represented in a two-dimensional space, obtained for the three runs considered. From these results, an analysis similar to that made for the single extrusion case can be carried out. Table 12 shows the optimal operating conditions for the first run, considering the best value for each of the objectives, while Table 13 shows the best location of the screw elements in the case of the second run and Tables 14 and 15 present the results for the third run. Note that all the solutions obtained resulted from a compromise between the three objectives considered simultaneously.

A comparison between the performance of the first and second runs is made in Table 17. Changing the operating conditions seems to be more effective for the objectives under analysis, since their values decrease from the first to the second run (values in bold). However, as expected, the most powerful approach to improve these objectives is given by the possibility of optimizing simultaneously the operating conditions and the screw configuration, as can be observed in Table 18. In this case, maximization of the average strain and minimization of the specific mechanical energy improve circa 27%, while the minimization of the viscous dissipation is mostly unaffected.

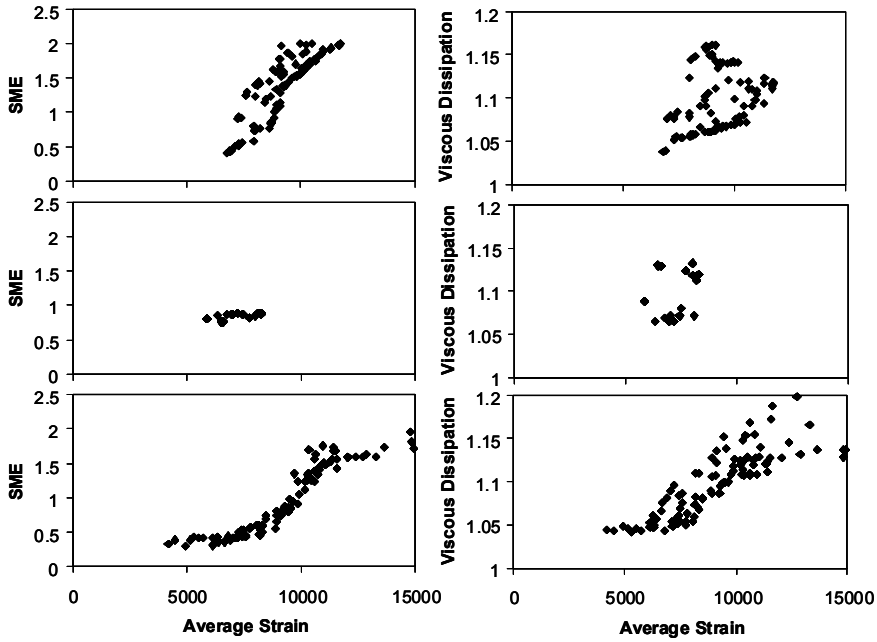

Figure 13. Pareto frontier for the optimization of: top) operating conditions; center) screw configuration; bottom) operating conditions and screw configuration - twin screw extrusion.

Table 12. Optimal operating conditions for the first run - twin screw extrusion.

Objective	Operating Conditions			Objectives		
	Q **(kg/hr)**	***N*** **(rpm)**	T_b **(°C)**	***AvgS***	***SME*** **(MJ/kg)**	***VD***
Max(AvgS)	4.7	156	182	11763	1.991	1.12
Min(SME)	6.5	71	240	6774	0.406	1.04
Min(VD)	6.5	71	240	6774	0.406	1.04

Table 13. Optimal screw configuration for the second run - twin screw extrusion.

Objective	Screw Element	3	4	5	6	7	8	9	10	11	12	13	14	15	16
Max(AvgS)	Length (mm)	30	30	30	60	30	45	60	60	37.5	30	120	60	30	120
	Pitch (mm)	60	30	KB -60º	45	20	KB -45º	30	20	KB -30º	-20	60	30	30	30
Min(SME)	Length (mm)	30	120	60	120	30	30	60	30	45	37.5	60	30	30	60
	Pitch (mm)	20	60	45	30	30	KB -60º	20	-20	KB -45º	KB -30º	30	30	60	30
Min(VD)	Length (mm)	30	30	30	30	60	30	60	120	60	45	60	120	30	37.5
	Pitch (mm)	KB -60º	30	-20	60	20	20	30	60	30	KB -45º	45	30	30	KB -30º

Table 15. Optimal operating conditions for the third run - twin screw extrusion.

Objective	Operating Conditions		
	Q (kg/hr)	N (rpm)	T_b (ºC)
Max(AvgS)	7.2	191	181
Min(SME)	9.6	77	236
Min(VD)	9.3	95	242

Table 16. Optimal screw configuration for the third run - twin screw extrusion.

Objective	Screw Element	3	4	5	6	7	8	9	10	11	12	13	14	15	16
Max(AvgS)	Length (mm)	37.5	30	30	60	30	60	120	30	120	30	60	30	45	60
	Pitch (mm)	KB -30º	30	60	45	KB -60º	30	60	30	30	-20	30	20	KB -45º	20
Min(SME)	Length (mm)	37.5	30	30	30	60	30	60	45	60	120	30	60	30	120
	Pitch (mm)	KB -30º	30	20	-20	30	KB -60º	20	KB -45º	30	60	60	45	30	30
Min(VD)	Length (mm)	60	30	30	30	60	60	30	37.5	120	120	45	60	30	30
	Pitch (mm)	20	-20	20	KB -60º	30	45	30	KB -30º	60	30	KB -45º	30	60	30

Table 17. Variation of the objectives between the first and second runs - twin screw extrusion.

Objective	Objectives			Objectives Variation (%)		
	AvgS	***SME* (MJ/kg)**	***VD***	***AvgS***	***SME* (MJ/kg)**	***VD***
Max(AvgS)	8269	0.890	1.12	**-29.7**	55.3	-0.1
Min(SME)	6469	0.759	1.13	-4.5	**-86.7**	-8.8
Min(VD)	635	0.857	1.06	-6.2	-110.9	**-2.6**

Table 18. Variation of the objectives between the first and third runs - twin screw extrusion.

Objective	Objectives			Objectives Variation (%)		
	AvgS	***SME* (MJ/kg)**	***VD***	***AvgS***	***SME* (MJ/kg)**	***VD***
Max(AvgS)	14940	1.718	1.14	**27.0**	13.7	-1.7
Min(SME)	4910	0.295	1.05	-27.5	**27.4**	-1.1
Min(VD)	5314	0.429	1.04	-21.5	-5.5	**-0.4**

4.4 Decision Making Strategies

In this section, the Decision Making (DM) strategies presented and discussed in Chapter 4 will be applied to Runs 1 and 5 of the single screw extrusion (Table 3). In each run, different sets of weights and a ε value of 0.1 (see Chapter 4 for more details) are used. The graph on top of Figure 14 is obtained for Run 1 without applying the DM, while that at the bottom results from using DM and three sets of weights. The methodology is clearly able to take into account the relative importance of the objectives: as the weight of the output decreases, the results converge to smaller output values.

Figure 15 presents the results of applying the DM strategy to run 5, dealing with 5 objectives, for two sets of weights. Again, when the importance of the output maximization objective decreases, the algorithm converges to smaller output values. Interestingly, the Pareto solutions are now concentrated in smaller regions in comparison with those initially obtained for run 5 (Figure 11). In any case, a smaller value of ε can be used to further reduce the region to be obtained.

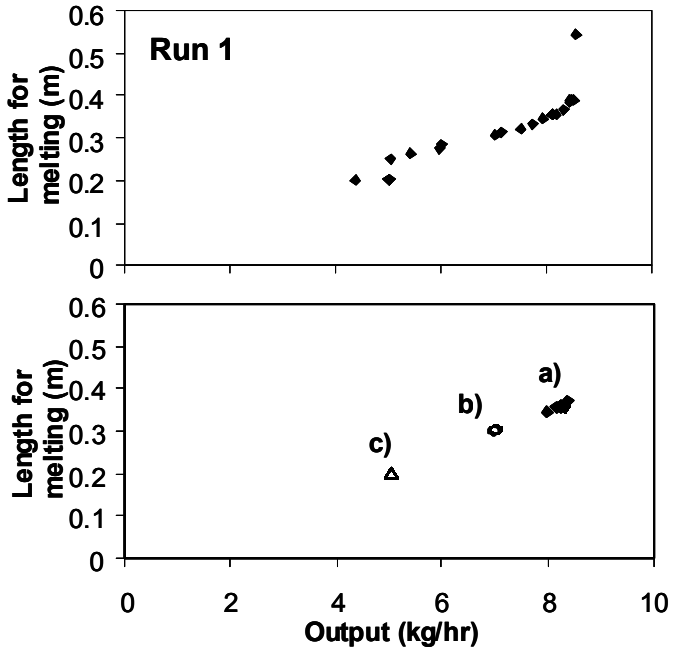

Figure 14. Pareto frontiers for Run 1 (top) and after application of the Decision Making strategy (bottom): a) w_i = (0.8;0.1); b) w_i = (0.5;0.5); c) w_i = (0.2;0.8) - single screw extrusion.

5 Conclusion

A MOEA was applied to solve single and co-rotating twin-screw extrusion optimization problems involving setting the operating conditions, designing screw(s), or both. These problems are often faced by process engineers and polymer compounders and are generally tackled on an empirical basis. Therefore, the chapter aimed at introducing a scientific method to solve efficiently an important class of practical technological problems.

The optimization methodology proposed here is able to solve problems with very distinct characteristics, from continuous to discrete decision variables and a mix of both. In the case of single extrusion, all variables are continuous; conversely, in the case of co-rotating twin-screw extrusion both situations can appear. The results generated for a few examples seem to be in agreement with current process knowledge (experimental validation is difficult

and costly for obvious reasons) and the solutions obtained are feasible and could be implemented in real extrusion practice. Finally, the DM strategy proposed in a separate chapter was applied here and showed good results.

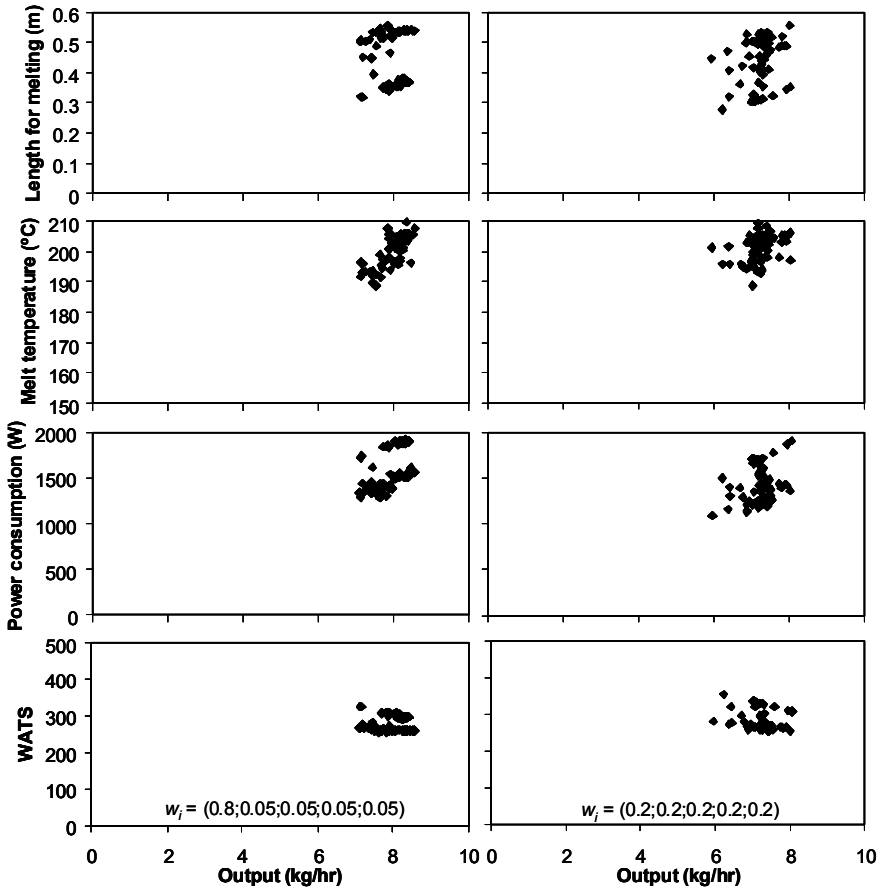

Figure 15. Pareto frontiers for Run 5 after application of the Decision Making strategy - single screw extrusion.

References

[1] Tadmor, Z.; Klein, I. *Engineering Principles of Plasticating Extrusion*. Van Nostrand Reinhold, New York,1970.

[2] Rauwendaal, C. *Polymer Extrusion*. Hanser Publishers, Munich,1986.

[3] Agassant J.F.; Avenas, P.; Sergent, J. *La Mise en Forme des Matiéres Plastiques*. Lavoisier, 3rd edition, Paris,1996.

[4] White, J.L. *Twin Screw Extrusion; Technology and Principles*. Hanser, Munich, 1990.

[5] Stevens, M.J.; Covas, J.A. *Extruder Principles and Operation*. 2nd ed., Chapman & Hall, London,1995.

[6] Covas, J.A. In *Rheological Fundamentals in Polymer Processing*. Covas, J.A. et al.; Ed.; Kluwer Academic Publishers, Dordrecht, 1995.

[7] O´Brian, K. *Computer Modelling for Extrusion and Other Continuous Polymer Processes*. Carl Hanser Verlag, Munich, 1992.

[8] Coello Coello, C.A.; Van Veldhuizen, D.A.; Lamont, G.B. *Evolutionary Algorithms for Solving Multi-Objective Problems*, Kluwer, 2002.

[9] Deb, K. *Multi-Objective Optimisation using Evolutionary Algorithms*. Wiley, New York, 2001.

[10] Gaspar-Cunha, A. *Modelling and Optimisation of Single Screw Extrusion*. PhD Thesis, University of Minho, Guimarães, Portugal, 2000.

[11] Gaspar-Cunha, A.; Covas, J.A. In *Metaheuristics for Multiobjective Optimisation*. Gandibleux, X. et al. (Ed.); Lecture Notes in Economics and Mathematical Systems, Springer, 2004.

[12] Covas, J.A.; Gaspar-Cunha, A.; Oliveira, P. *Polym. Eng. Sci.* 1999, 39, 443-456.

[13] Gaspar-Cunha, A.; Poulesquen, A.; Vergnes, B.; Covas, J.A. *Intern. Polym. Process.* 2002, 17, 201-213.

[14] Gaspar-Cunha, A.; Covas, J.A. In *Applications of Multi-Objective Evolutionary Algorithms*, Coello Coello, C.A.; Lamont, G.B.; Ed; World Scientific, Singapore, 2005, pp. 177-197,.

[15] Walker, D.M. *Chem. Eng. Sci.* 1966, 21, 975-997.

[16] Broyer, E.; Tadmor, Z. *Polym. Eng. Sci.* 1972, 12, 12-24.

[17] Tadmor, Z.; Broyer, E. *Polym. Eng. Sci.* 1972, 12, 378-386.

[18] Kacir, L.; Tadmor, Z. *Polym. Eng. Sci.* 1972, 12, 387-395.

[19] Lindt, J.T.; Elbirli, B. *Polym. Eng. Sci*. 1985, 25, 412-418.

[20] Elbirli, B.; Lindt, J.T.; Gottgetreu, S.R.; Baba, S.M. *Polym. Eng. Sci*. 1984, 24, 988- 999.

[21] Pinto, G.; Tadmor, Z. *Polym. Eng. Sci.* 1970, 10, 279-288.

[22] Bigg, D.M. *Mixing in a Single Screw Extruder*, Ph. D. Thesis, University of Massachusetts,1973.

[23] Booy, M. L. *Polym. Eng. Sci.* 1978, 18, 973-984.

[24] Potente, H.; Melisch, U. *International Polymer Processing*. 11, 101-108.

[25] Teixeira, C.; Faria, R.; Covas, J.A.; Gaspar-Cunha, A. In 10th Esaform Conference on Material Forming, Cueto, E.; Chinesta, F.; Ed.; Zaragoza, Spain, 2007.

[26] Vergnes, B.; Della Valle, G.; Delamare, L. Polym. Eng. Sci. 1998, 38, 1781-1792.

[27] Gogos, C.G.; Tadmor, Z.; Kim, M.O. *Advances in Polymer Technology*. 1998, 17, 285-305.

[28] Vergnes, B.; Souveton, MG.; Delacour, M.L.; Ainser, A. *International Polymer Processing*. 2001, 16, 351-362.

[29] Zhu, L.; Narh, K.A.; Geng, X. *Journal of Polymer Science: Part B*. 2001, 39, 2462-2468.

[30] Covas, J.A.; Gaspar-Cunha, A. *Plastics, Rubber and Composites: Macromolecular Engineering*. 2004, 33, 416-425.

[31] Gaspar-Cunha, A.; Vergnes, B.; Covas, J.A. *Polym. Eng. Sci.* 2005, 45, 1159-1173.

[32] Teixeira, C.; Covas, J.A.; Stützle, T. Gaspar-Cunha, A.; International Transitions in Operational Research, In press, 2010.

[33] Tao, G.; Michalewicz, Z. In *Proceedings of the 5th Parallel Problem Solving from Nature*, Amsterdam, 1998, pp. 803-811.

[34] Teixeira, C.; Covas, J.A.; Stützle, T. Gaspar-Cunha, A.; In Soft Computing in Industrial Applications; Gao, X.-Z.; Gaspar-Cunha, A.; Köppen, M.; Schaefer, G.; Wang, J.; Ed.; Advances in Intelligence and Soft Computing Series, Springer, Berlin, 2010, Vol. 75, pp. 3-10.